

HUBBLE SPACE TELESCOPE WFC3 GRISM SPECTROSCOPY AND IMAGING OF A GROWING COMPACT GALAXY  
AT  $Z = 1.9$ PIETER G. VAN DOKKUM AND GABRIEL BRAMMER  
Department of Astronomy, Yale University, New Haven, CT 06520-8101  
*draft, November 4, 2018*

## ABSTRACT

We present HST/WFC3 grism spectroscopy of the brightest galaxy at  $z > 1.5$  in the GOODS-South WFC3 Early Release Science grism pointing, covering the wavelength range  $0.9\,\mu\text{m} - 1.7\,\mu\text{m}$ . The spectrum is of remarkable quality and shows the redshifted Balmer lines  $H\beta$ ,  $H\gamma$ , and  $H\delta$  in absorption at  $z = 1.902 \pm 0.002$ , correcting previous erroneous redshift measurements from the rest-frame UV. The average rest-frame equivalent width of the Balmer lines is  $8\,\text{\AA} \pm 1\,\text{\AA}$ , which can be produced by a post-starburst stellar population with a luminosity-weighted age of  $\approx 0.5\,\text{Gyr}$ . The  $M/L$  ratio inferred from the spectrum implies a stellar mass of  $(4 \pm 1) \times 10^{11} M_{\odot}$ . We determine the morphology of the galaxy from a deep WFC3  $H_{160}$  image. Similar to other massive galaxies at  $z \sim 2$  the galaxy is compact, with an effective radius of  $2.1 \pm 0.3\,\text{kpc}$ . Although most of the light is in a compact core, the galaxy has two red, smooth spiral arms that appear to be tidally-induced. The spatially-resolved spectroscopy demonstrates that the center of the galaxy is quiescent and the surrounding disk is forming stars, as it shows  $H\beta$  in emission. The galaxy is interacting with a companion at a projected distance of  $18\,\text{kpc}$ , which also shows prominent tidal features. The companion has a slightly redder spectrum than the primary galaxy but is a factor of  $\sim 10$  fainter and may have a lower metallicity. It is tempting to interpret these observations as “smoking gun” evidence for the growth of compact, quiescent high redshift galaxies through minor mergers, which has been proposed by several recent observational and theoretical studies. Interestingly both objects host luminous AGNs, as indicated by their X-ray luminosities, which implies that these mergers can be accompanied by significant black hole growth. This study illustrates the power of moderate dispersion, low background near-IR spectroscopy at HST resolution, which is now available with the WFC3 grism.

*Subject headings:* cosmology: observations — galaxies: evolution — galaxies: formation

## 1. INTRODUCTION

The formation history of massive galaxies is not well understood. Present-day galaxies with stellar masses  $\gtrsim 3 \times 10^{11} M_{\odot}$  are typically giant elliptical galaxies in the centers of galaxy groups. These galaxies have old stellar populations and follow tight scaling relations between their velocity dispersions, sizes, surface brightnesses, line strengths, and other parameters (e.g., Djorgovski & Davis 1987; Thomas et al. 2005). At redshifts  $z \sim 2$  massive galaxies form a more complex population. A fraction of the population is forming stars at a high rate, as determined from their brightness in the rest-frame UV or IR, emission lines such as  $H\alpha$ , and other indicators (e.g., Steidel et al. 1996; Blain et al. 2002; Rubin et al. 2004; Papovich et al. 2006, and many other studies). However, others have no clear indications of ongoing star formation and have spectral energy distributions (SEDs) characterized by strong Balmer- or  $4000\,\text{\AA}$  breaks (e.g., Daddi et al. 2005; Kriek et al. 2006). The existence of these “quiescent” galaxies at this early epoch is in itself remarkable, and provides constraints on the accretion and thermodynamics of gas in massive halos at  $z > 2$  (e.g., Kereš et al. 2005; Dekel & Birnboim 2006). What is perhaps even more surprising is that these galaxies are structurally very different from early-type galaxies in the nearby Universe: their effective radii are typically  $1\text{--}2\,\text{kpc}$ , much smaller than nearby giant ellipticals (e.g., Daddi et al. 2005; Trujillo et al. 2006; van Dokkum et al. 2008; Cimatti et al. 2008).

Several explanations have been offered for the dramatic size difference between local massive galaxies and quiescent galaxies at high redshift. The simplest is that observers underestimated the sizes and/or overestimated the masses. Al-

though subtle errors are almost certainly present in the interpretation of the data, recent studies suggest that it is difficult to change the sizes and the masses by more than a factor of 1.5, unless the IMF is altered (e.g., Muzzin et al. 2009; Casata et al. 2010; Szomoru et al. 2010). Other explanations include extreme mass loss due to a quasar-driven wind (Fan et al. 2008), strong radial age gradients leading to large differences between mass-weighted and luminosity-weighted ages (Hopkins et al. 2009; La Barbera & de Carvalho 2009), star formation due to gas accretion (Franx et al. 2008), and selection effects (e.g., van Dokkum et al. 2008; van der Wel et al. 2009). Perhaps the most plausible mechanism for bringing the compact  $z \sim 2$  galaxies onto the local mass-size relation is (minor) merging (e.g., Bezanson et al. 2009; Naab, Johansson, & Ostriker 2009; van Dokkum et al. 2010; Carrasco, Conselice, & Trujillo 2010). Numerical simulations predict that such mergers are frequent (Guo & White 2008; Naab et al. 2009); furthermore, they may lead to stronger size growth than mass growth (Bezanson et al. 2009). From an analysis of mass evolution at fixed number density, van Dokkum et al. (2010) infer that massive galaxies have doubled their mass since  $z = 2$ , and suggest that  $\sim 80\%$  of this mass growth can be attributed to mergers.

Although qualitatively consistent with observations and theory the minor merger scenario currently has little direct evidence to support it. It is also not clear whether properties other than sizes and masses are easily explained in this context; one of the open questions is why present-day elliptical galaxies are so red and homogeneous if half of their mass was accreted from the general field at relatively recent times. Ideally we would identify and study the infalling population directly at high redshift, but so far this has been hampered by

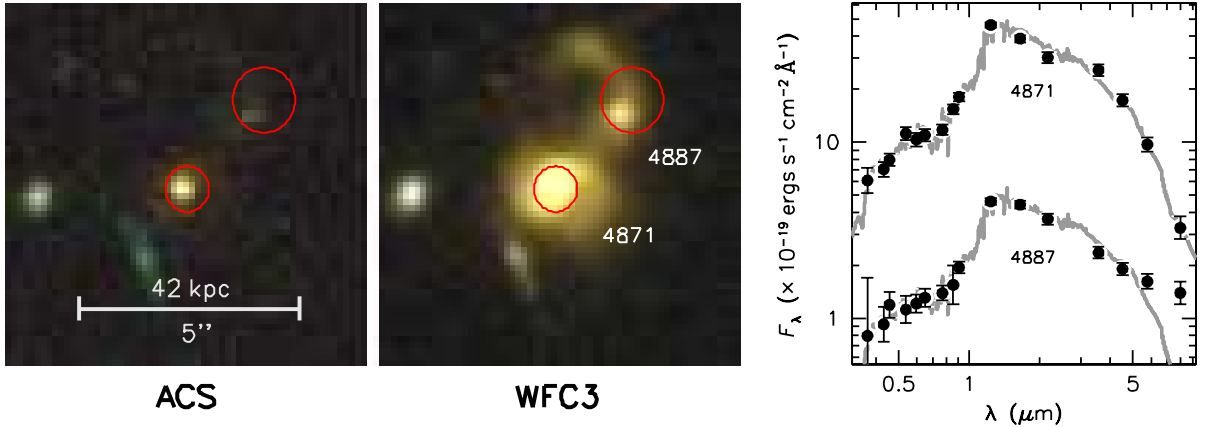


FIG. 2.— HST ACS and WFC3 images of FW-4871 and its companion FW-4887. The ACS color image was created from the  $B_{435}$ ,  $V_{606}$ , and  $z_{850}$  bands, and the WFC3 image from the  $Y_{098}$ ,  $J_{125}$ , and  $H_{160}$  bands. FW-4871 has a compact core and spiral arms, which may be the result of an interaction with FW-4887. Red circles are the locations of X-ray sources in the Luo et al. (2008) catalog, with the size of the circles indicating the uncertainties in the positions. Both galaxies host an AGN. The SEDs of the two galaxies (from Wuyts et al. 2008) are shown in the right-most panel. The galaxies are both red and have broadly similar SEDs.

the limitations of ground-based spectroscopy and ground- and space-based near-IR imaging.

In this *Letter*, we use the exquisite WFC3 grism on the *Hubble Space Telescope* (HST), in combination with WFC3 imaging, to study the environment of a quiescent compact galaxy at  $z = 1.9$ . As we show below, the observations presented here provide the first direct evidence for minor mergers as a mechanism for the growth of compact galaxies at high redshift. We use  $H_0 = 70 \text{ km s}^{-1} \text{ Mpc}^{-1}$ ,  $\Omega_m = 0.3$ , and  $\Omega_\Lambda = 0.7$ . Magnitudes are on the AB system.

## 2. SELECTION AND BASIC DATA

The Early Release Science (ERS) WFC3 imaging observations of the GOODS-South field comprise a mosaic of eight HST pointings. All eight pointings were observed with a suite of imaging filters but only one was observed with the G102 and G141 grisms. The grism data are important for measuring the redshifts, ages, and star formation rates of massive galaxies at high redshift and indispensable for measuring the redshifts of any faint companion galaxies. The G141 grism is particularly useful as it is very sensitive and its wavelength range of  $1.1 \mu m - 1.7 \mu m$  covers the redshifted Balmer lines, 4000 Å break, and [O III] emission at  $z \sim 2$ . Here we concentrate on the brightest galaxy at  $z > 1.5$  in the  $2' \times 2'$  grism field, indicated with the arrow in Fig. 1. The galaxy has ID number 4871 in the  $K$ -selected FIREWORKS catalog of GOODS-South (Wuyts et al. 2008), and has a total  $K$  magnitude of 19.7.

ACS and WFC3 color images of the galaxy are shown in Fig. 2, along with the SED from the Wuyts et al. catalog. The galaxy is faint and unremarkable in the ACS bands but very bright in the WFC3 images, owing to its red SED. It is composed of a compact core in addition to diffuse spiral arms, which appear to originate from a tidal interaction with a companion galaxy, object FW-4887 in the FIREWORKS catalog. The companion has a similar SED as 4871 but is a factor of  $\sim 10$  fainter at  $K = 22.0$ . It has a  $2''$  long tidal tail, extending away from FW-4871.

Interestingly, both FW-4871 and FW-4887 are X-ray sources (Luo et al. 2008, ID numbers 145 and 142 respectively). Their X-ray luminosities are  $6.4 \times 10^{43} \text{ ergs s}^{-1}$  and  $3.5 \times 10^{43} \text{ ergs s}^{-1}$  respectively, where we used the full-band fluxes from Luo et al. (2008) and the redshift derived be-

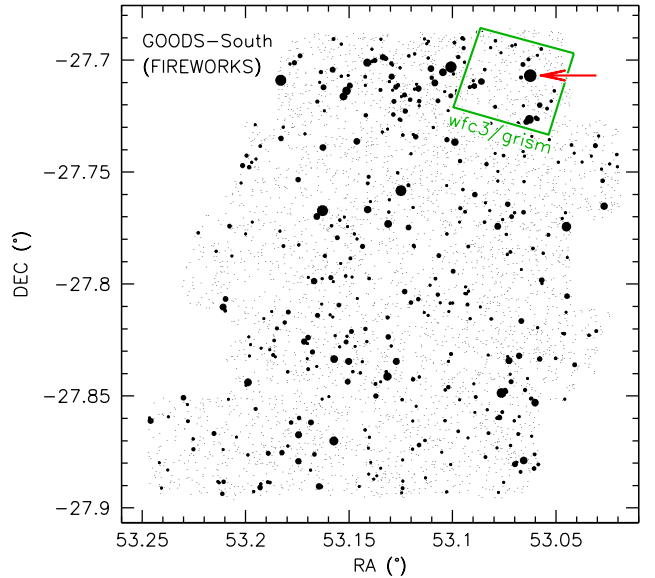


FIG. 1.— Galaxies in the GOODS-South field, from the FIREWORKS catalog (Wuyts et al. 2008). Filled circles are galaxies at  $z > 1.5$ , with the size of the circle indicating the brightness in the  $K$  band. The green box shows the location of the single HST/WFC3 G141 grism exposure that has been obtained as part of the WFC3 ERS. The arrow indicates the brightest galaxy at  $z > 1.5$  in this pointing, object FW-4871 in the Wuyts et al. catalog.

low. These luminosities would imply star formation rates  $\gg 1000 M_\odot \text{ yr}^{-1}$  (Ranalli, Comastri, & Setti 2003), and we conclude that both galaxies almost certainly host an active galactic nucleus (AGN). The AGN in the companion galaxy is likely heavily obscured: FW-4887 has an  $8 \mu m$  “upturn” (see Fig. 2) and is a very bright MIPS  $24 \mu m$  source with a flux density of  $0.4 \text{ mJy}$  (Wuyts et al. 2008).

FW-4871 has been targeted several times for optical spectroscopy. Three spectroscopic redshifts are available, all from the GOODS-VIMOS survey:  $z = 0.352$ ,  $z = 2.494$ , and  $z = 2.609$ , with qualities C, C, and B respectively (Popesso et al. 2009; Balestra et al. 2010). As we show below all three redshifts are incorrect.

### 3. HST WFC3 GRISM SPECTROSCOPY

The field was observed with the G102 and G141 grisms, providing continuous wavelength coverage from 0.8–1.7  $\mu\text{m}$  for all objects in the  $2' \times 2'$  WFC3/IR field of view. Each grism image has a total integration time of 4212 s, divided over four dithered exposures in two orbits. We reduced the grism observations and extracted spectra using a combination of standard `pyraf` tasks (e.g., `multidriz`), the `aXe` package (Kümmel et al. 2009), and custom scripts to improve background subtraction and optimize the extraction apertures (see, e.g., Pirzkal et al. 2004). The wavelength calibration and extraction apertures for G102 and G141 are based on undispersed images in  $Y_{098}$  and  $H_{140}$  respectively. These direct images were obtained at the same dither positions as the dispersed data.

The grism spectrum of FW-4871 is shown in Fig. 3; it is of very high quality with  $S/N \approx 90$  per 47  $\text{\AA}$  pixel at 1.2  $\mu\text{m}$ . The galaxy has strong  $H\beta$ ,  $H\gamma$ , and  $H\delta$  absorption lines, and a pronounced Balmer break. The redshift  $z = 1.902 \pm 0.002$ . The  $[\text{O III}]$  lines are undetected; the upper limit on their rest-frame equivalent width is  $\lesssim 2 \text{\AA}$ . Note that these lines (and  $H\beta$ ) are completely inaccessible from the ground, as they fall in between the  $J$  and  $H$  atmospheric windows. The average rest-frame equivalent width of  $H\beta$ ,  $H\gamma$ , and  $H\delta$  is  $8 \text{\AA} \pm 1 \text{\AA}$ , which implies that a post-starburst population dominates the rest-frame optical light.

We fitted the spectrum with Bruzual & Charlot (2003) stellar population synthesis models (see, e.g., Kriek et al. 2009). Good fits are obtained for populations with low star formation rates at the epoch of observation but relatively young luminosity-weighted ages ( $\approx 0.5$  Gyr), combined with a moderate amount of dust ( $A_V \sim 1$ ). Adopting simple top-hat star formation histories, we find that the data can be fit with an extreme burst of  $\sim 5000 \text{ M}_\odot \text{ yr}^{-1}$  at  $z \sim 2.2$  (purple), or with a star formation rate of  $\sim 500 \text{ M}_\odot \text{ yr}^{-1}$  sustained over  $\sim 1$  Gyr (orange). In the latter model the star formation truncated only 150 Myr prior to the epoch of observation, comparable to the dynamical time at the distance of the companion galaxy. Models with less dust and higher luminosity-weighted ages do not fit the spectrum well as they have stronger  $\text{Ca H+K}$  and weaker  $H\delta$  absorption than is observed; as an example, the red model in Fig. 3 has a luminosity-weighted age of 1 Gyr and  $A_V = 0.3$  and is a poor fit to the spectrum. Scaling the models to the total magnitudes given in Wuyts et al. (2008) we find that the stellar mass of FW-4871 is  $(4 \pm 1) \times 10^{11} \text{ M}_\odot$  for a Chabrier (2003) IMF.

We also extracted a spectrum of the companion galaxy from the grism data, even though it is quite faint at  $H = 22.4$ . As can be seen in Fig. 3 we clearly detect the continuum, thanks to the low background from space and the lack of sky lines. The galaxy has a continuum break in the same wavelength region as FW-4871 and shows oxygen lines and  $H\beta$  in emission. Its redshift of  $z = 1.898 \pm 0.003$  is consistent with that of FW-4871, demonstrating that the two are associated. Assuming that the  $H\beta$  emission is due to star formation we derive a star formation rate of order  $5 - 10 \text{ M}_\odot \text{ yr}^{-1}$  (Kennicutt 1998, for  $A_V = 1 - 2$  mag). Interestingly, the spectrum of the companion galaxy is redder than that of FW-4871, although this is difficult to quantify due to contamination of its spectrum from a nearby object. This may be caused by dust and/or the presence of an old stellar population.

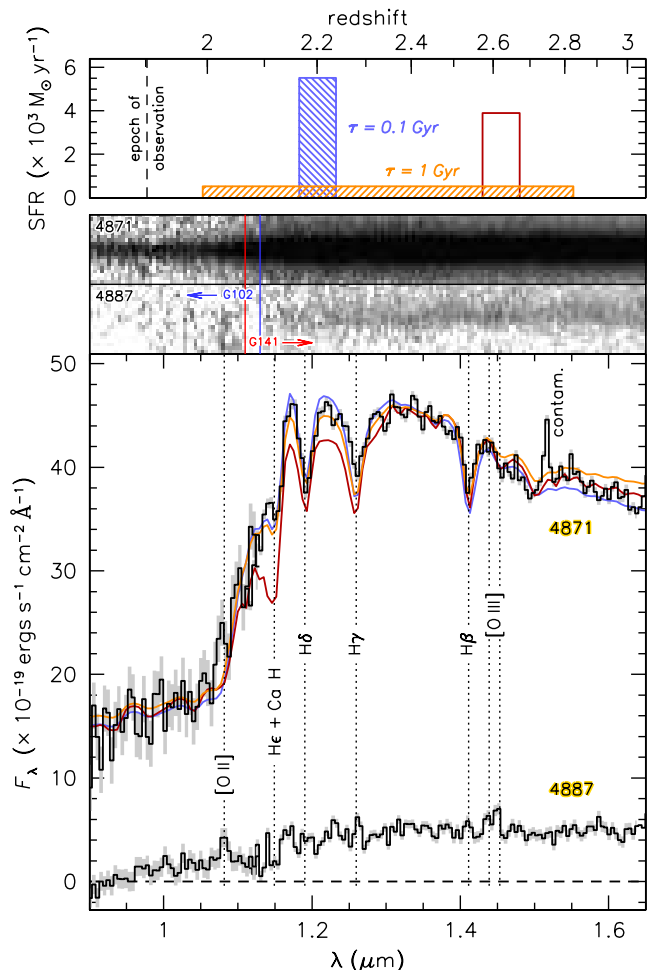


FIG. 3.— HST/WFC3 G102 and G141 grism spectra of FW-4871 and its companion. The spectrum of FW-4871 is dominated by A stars, and shows prominent Balmer absorption lines. The orange and purple lines are stellar populations with a luminosity-weighted age of 0.5 Gyr,  $A_V \sim 1$ , and a redshift  $z = 1.902$ . The data are consistent with a short, intense burst at  $z = 2.2$  or a more extended star formation history. The red model has a luminosity-weighted age of 1 Gyr and less dust; this model can be ruled out. The feature at 1.51  $\mu\text{m}$  is a contaminating emission line from an unrelated galaxy. The spectrum of FW-4887 also shows a continuum break, along with emission lines of  $[\text{O II}] \lambda 3727$ ,  $H\beta$ , and  $[\text{O III}] \lambda 4959, 5007$  at approximately the same redshift as FW-4871.

### 4. STRUCTURE AND SPATIALLY-RESOLVED SPECTROSCOPY

As discussed in § 1, massive quiescent galaxies at  $z \sim 2$  typically have very small sizes. Despite its spiral arms this is also the case for FW-4871, as most of its light comes from a compact core. We quantified this by fitting Sérsic (1968) models to the  $H_{160}$  image using `galfit` (Peng et al. 2002). Other objects in the field, including the companion galaxy, were masked in the fit. The fit and the residuals are shown in Fig. 4. The asymmetric spiral pattern is a striking feature in the residual image. The best-fit Sérsic index  $n = 3.7 \pm 0.3$  and the best-fit effective radius  $r_e = 0''.25 \pm 0''.03$ , corresponding to  $2.1 \pm 0.3$  kpc. The formal errors are very small; the quoted uncertainties indicate the full range of solutions obtained when using different stars in the field as PSFs, but do not include other sources of systematic error.

The S/N of the grism data is sufficiently high that we can

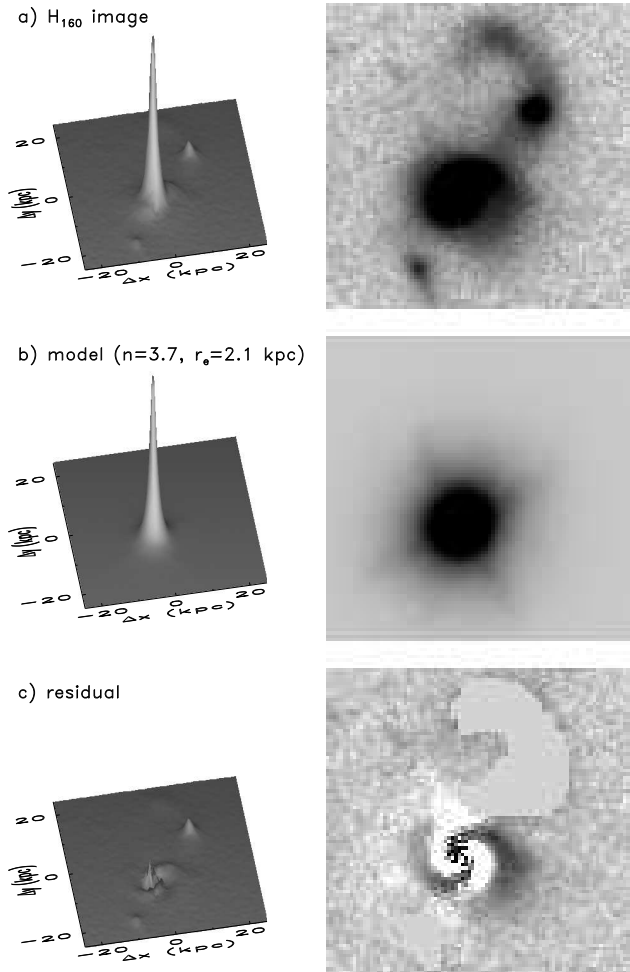


FIG. 4.— Seric fits to the  $H_{160}$  image of FW-4871, which was drizzled to a pixel scale of  $0''.065$ . The galaxy image (a), the best-fitting model (b), and the residual (c) are shown. The 3D plots illustrate that most of the light is in a compact core. The residual image shows a regular two-armed spiral, which may have been induced by a tidal interaction.

compare the spectrum of the core to that at larger radii. As shown in Fig. 5 the average spectrum of the inner 4 pixels ( $r \leq 0''.13$ ) is similar to that at large radii ( $0''.13 < r < 0''.65$ ), with the notable exception of  $H\beta$ : it is undetected away from the center, which implies that it is filled in by emission. We demonstrate this by subtracting the Bruzual & Charlot (2003) model shown in Fig. 3 from both the central spectrum and the outer spectrum. The spectrum of the inner parts shows no systematic residuals, but the spectrum away from the center shows a positive residual at the wavelength of  $H\beta$ . We infer that FW-4871 is not entirely “dead” but is forming stars in the spiral arms. The amount of star formation is difficult to quantify and depends on the assumed reddening; assuming  $E(B-V) \sim 0.3$  it is  $\sim 20 M_{\odot} \text{ yr}^{-1}$ .

## 5. DISCUSSION

The WFC3 grism and imaging data of FW-4871 may provide “smoking gun” evidence for minor mergers as an important growth mechanism of massive galaxies: FW-4871 is a massive, compact galaxy at  $z \sim 2$  which is interacting with

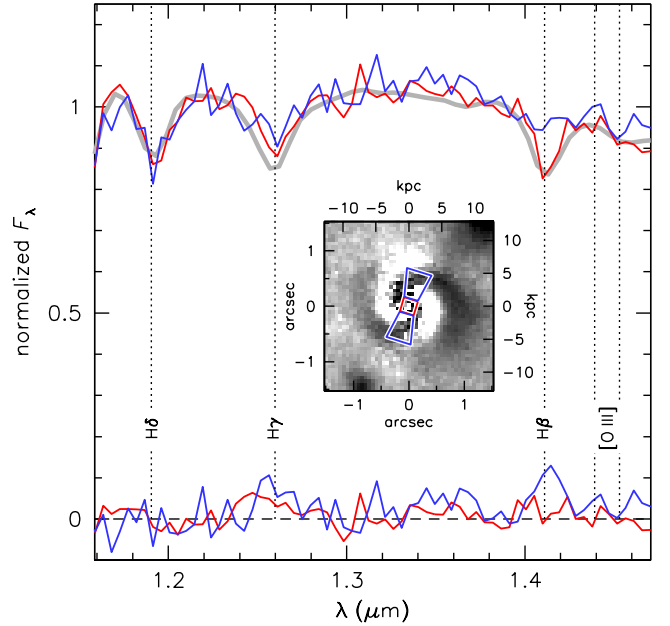


FIG. 5.— Spatially-resolved Balmer lines. The red spectrum is for the central  $r < 0''.13$  of FW-4871 ( $r < 1$  kpc) and the blue spectrum is for radii  $0''.13 < r < 0''.65$ . Residual spectra, obtained by subtracting the (light grey) model from the data, are also shown. At large radii  $H\beta$  is filled in by emission, possibly due to star formation associated with the spiral arms. The non-detection of [O III] (and [O II], which is not shown) suggests a high metallicity for the gas in these regions.

a  $\sim 10\times$  less massive companion. The quiescent spectrum of the primary galaxy is qualitatively consistent with the spectra of other compact high redshift galaxies and with the old stellar ages of present-day early-type galaxies. This mode of growth has been proposed by several recent studies to explain the size difference between massive galaxies at high redshift and low redshift (e.g., Bezanson et al. 2009; Naab et al. 2009).

Nearby ellipticals have gradients in their color and metallicity, such that they are bluer and more metal-poor at larger radii (e.g., Franx, Illingworth, & Heckman 1989). Interestingly, we can begin to address the origin of these gradients with the kind of data that we are now getting from HST. The relatively strong oxygen lines and weak  $H\beta$  of the infalling galaxy imply  $\log R_{23} \sim 1$ , and a metallicity that is  $\gtrsim 1/3$  times the Solar value (Pilyugin & Thuan 2005). The spectrum extracted from the disk of FW-4871 has, by contrast, no detected oxygen lines and an unambiguous detection of  $H\beta$ . It has  $\log R_{23} \lesssim 0$ , which implies a Solar or super-Solar metallicity. Qualitatively these results are consistent with the idea that the metallicity gradients of elliptical galaxies reflect a gradual increase with radius in the fraction of stars that came from infalling low-mass satellites.

The apparent absence of star formation in the central regions of FW-4871 might be related to its active nucleus. It has been suggested by many authors that AGN could prevent gas cooling and star formation (e.g., Croton et al. 2006) and in this context the observed properties of FW-4871, such as the lower limit on the ratio of its X-ray luminosity to [O III] and  $H\beta$ , may provide constraints on the mechanism(s) of AGN feedback (see also Fiore et al. 2008; Kriek et al. 2007, 2009). In any case, the fact that both interacting galaxies host an AGN is remarkable, as it demonstrates that their black holes are undergoing a “growth spurt” prior to their merger. We

note here that the only indication of the AGNs in the optical and near-IR is a faint emission line in the VIMOS spectra of FW-4871, which we now identify<sup>1</sup> as C IV.

There are several important caveats, uncertainties, and complications. First, FW-4871 is not only growing through the accretion of FW-4887, but also through star formation. There is evidence for star formation in the companion (although its emission lines could be influenced by its active nucleus) and also in the spiral arms of FW-4871. In most models such “residual” star formation takes place in the center of the most massive galaxy (see, e.g., Naab et al. 2009), but that is in fact the only place where we do *not* see evidence for star formation. We note, however, that because of the large mass of FW-4871 the specific star formation rate of the entire system is low at  $\text{SFR}/M_{\text{stellar}} \lesssim 10^{-10} \text{ yr}^{-1}$ .

Second, although the spectrum of FW-4871 resembles those of the compact galaxies studied in Kriek et al. (2006) and van Dokkum et al. (2008), the galaxy formed its stars at significantly lower redshift. As shown in § 3 its star formation rate probably was  $\sim 500 M_{\odot} \text{ yr}^{-1}$  as recently as 150 Myr prior to the epoch of observation, i.e., at  $z \approx 2$ . It is therefore not a direct descendant of quiescent galaxies at  $z \sim 2.3$ . Interestingly, star forming galaxies at  $z > 2$  are typically larger than FW-4871 in the rest-frame optical (e.g., Toft et al. 2007), which may imply that FW-4871 is unusual or that a significant fraction of the star formation in massive galaxies at  $z \sim 2.5$  takes place in heavily obscured, compact regions.

<sup>1</sup> The three erroneous redshifts for FW-4871 were not due to a misidentification of this line; the line was not recognized as a real feature in

Third, the fact that the time since the truncation of star formation is similar to the dynamical time calls into question whether we are witnessing a “two-stage” galaxy formation process, with steady accretion of satellite galaxies following an initial highly dissipational star formation phase (e.g., Naab et al. 2009; Dekel et al. 2009). An alternative interpretation is that the companion galaxy is somehow related to the truncation, for example by triggering the AGN in FW-4871  $\sim 150$  Myr ago. Numerical simulations that aim to reproduce both the 2D spectrum and the morphological features might shed some light on these issues.

As illustrated in this *Letter* the WFC3 camera on HST has opened up a new regime of detailed spectroscopic and imaging studies of high redshift galaxies. The quality of the rest-frame optical continuum spectra shown in Fig. 3 greatly exceeds what can be achieved from the ground (see, e.g., Kriek et al. 2009), and the grism provides simultaneous spectroscopy of all 200-300 objects with  $H \lesssim 23$  in the WFC3 field. Future WFC3 spectroscopic and imaging surveys over large areas have the potential to robustly measure the evolution of galaxies over the redshift range  $1 < z < 3$ .

We thank the WFC3 ERS team for their exciting program and Marijn Franx, Hans-Walter Rix, Mariska Kriek, Katherine Whitaker, and Anna Pasquali for comments.

the GOODS-VIMOS analysis of the VIMOS spectrum.

## REFERENCES

- Balestra, I., Mainieri, V., Popesso, P., Dickinson, M., Nonino, M., Rosati, P., Teimoorinia, H., Vanzella, E., et al. 2010, *ArXiv e-prints*
- Bezanson, R., van Dokkum, P. G., Tal, T., Marchesini, D., Kriek, M., Franx, M., & Coppi, P. 2009, *ApJ*, 697, 1290
- Blain, A. W., Smail, I., Ivison, R. J., Kneib, J.-P., & Frayer, D. T. 2002, *Phys. Rep.*, 369, 111
- Bruzual, G. & Charlot, S. 2003, *MNRAS*, 344, 1000
- Carrasco, E. R., Conselice, C. J., & Trujillo, I. 2010, *MNRAS*, in press (arXiv:1003.1956)
- Cassata, P., et al. 2010, *ApJL*, in press (arXiv:0911.1158)
- Chabrier, G. 2003, *PASP*, 115, 763
- Cimatti, A., Cassata, P., Pozzetti, L., Kurk, J., Mignoli, M., Renzini, A., Daddi, E., Bolzonella, M., et al. 2008, *A&A*, 482, 21
- Croton, D. J., Springel, V., White, S. D. M., De Lucia, G., Frenk, C. S., Gao, L., Jenkins, A., Kauffmann, G., et al. 2006, *MNRAS*, 365, 11
- Daddi, E., Renzini, A., Pirzkal, N., Cimatti, A., Malhotra, S., Stiavelli, M., Xu, C., Pasquali, A., et al. 2005, *ApJ*, 626, 680
- Dekel, A. & Birnboim, Y. 2006, *MNRAS*, 368, 2
- Dekel, A., Birnboim, Y., Engel, G., Freundlich, J., Goerdt, T., Mumcuoglu, M., Neistein, E., Pichon, C., et al. 2009, *Nature*, 457, 451
- Djorgovski, S. & Davis, M. 1987, *ApJ*, 313, 59
- Fan, L., Lapi, A., De Zotti, G., & Danese, L. 2008, *ApJ*, 689, L101
- Fiore, F., Grazian, A., Santini, P., Puccetti, S., Brusa, M., Feruglio, C., Fontana, A., Giallongo, E., et al. 2008, *ApJ*, 672, 94
- Franx, M., Illingworth, G., & Heckman, T. 1989, *AJ*, 98, 538
- Franx, M., van Dokkum, P. G., Schreiber, N. M. F., Wuyts, S., Labbé, I., & Toft, S. 2008, *ApJ*, 688, 770
- Guo, Q. & White, S. D. M. 2008, *MNRAS*, 384, 2
- Hopkins, P. F., Hernquist, L., Cox, T. J., Keres, D., & Wuyts, S. 2009, *ApJ*, 691, 1424
- Kennicutt, R. C. 1998, *ARA&A*, 36, 189
- Kereš, D., Katz, N., Weinberg, D. H., & Davé, R. 2005, *MNRAS*, 363, 2
- Kriek, M., van Dokkum, P. G., Franx, M., Illingworth, G. D., Coppi, P., Förster Schreiber, N. M., Gawiser, E., Labbé, I., et al. 2007, *ApJ*, 669, 776
- Kriek, M., van Dokkum, P. G., Franx, M., Quadri, R., Gawiser, E., Herrera, D., Illingworth, G. D., Labbé, I., et al. 2006, *ApJ*, 649, L71
- Kriek, M., van Dokkum, P. G., Labbé, I., Franx, M., Illingworth, G. D., Marchesini, D., & Quadri, R. F. 2009, *ApJ*, 700, 221
- Kümmel, M., Walsh, J. R., Pirzkal, N., Kuntschner, H., & Pasquali, A. 2009, *PASP*, 121, 59
- La Barbera, F. & de Carvalho, R. R. 2009, *ApJ*, 699, L76
- Luo, B., Bauer, F. E., Brandt, W. N., Alexander, D. M., Lehmer, B. D., Schneider, D. P., Brusa, M., Comastri, A., et al. 2008, *ApJS*, 179, 19
- Muzzin, A., van Dokkum, P., Franx, M., Marchesini, D., Kriek, M., & Labbé, I. 2009, *ApJ*, 706, L188
- Naab, T., Johansson, P. H., & Ostriker, J. P. 2009, *ApJ*, 699, L178
- Papovich, C., Moustakas, L. A., Dickinson, M., Le Floc’h, E., Rieke, G. H., Daddi, E., Alexander, D. M., Bauer, F., et al. 2006, *ApJ*, 640, 92
- Peng, C. Y., Ho, L. C., Impey, C. D., & Rix, H.-W. 2002, *AJ*, 124, 266
- Pilyugin, L. S. & Thuan, T. X. 2005, *ApJ*, 631, 231
- Pirzkal, N., Xu, C., Malhotra, S., Rhoads, J. E., Koekemoer, A. M., Moustakas, L. A., Walsh, J. R., Windhorst, R. A., et al. 2004, *ApJS*, 154, 501
- Popesso, P., Dickinson, M., Nonino, M., Vanzella, E., Daddi, E., Fosbury, R. A. E., Kuntschner, H., Mainieri, V., et al. 2009, *A&A*, 494, 443
- Ranalli, P., Comastri, A., & Setti, G. 2003, *A&A*, 399, 39
- Rubin, K. H. R., van Dokkum, P. G., Coppi, P., Johnson, O., Förster Schreiber, N. M., Franx, M., & van der Werf, P. 2004, *ApJ*, 613, L5
- Sersic, J. L. 1968, *Atlas de galaxias australes* (Cordoba, Argentina: Observatorio Astronomico, 1968)
- Steidel, C. C., Giavalisco, M., Pettini, M., Dickinson, M., & Adelberger, K. L. 1996, *ApJ*, 462, L17
- Szomoru, D., Franx, M., van Dokkum, P. G., Trenti, M., Illingworth, G., & Labbé, I. 2010, *ApJL*, submitted
- Thomas, D., Maraston, C., Bender, R., & Mendes de Oliveira, C. 2005, *ApJ*, 621, 673
- Toft, S., van Dokkum, P., Franx, M., Labe, I., Förster Schreiber, N. M., Wuyts, S., Webb, T., Rudnick, G., et al. 2007, *ApJ*, 671, 285
- Trujillo, I., et al. 2006, *MNRAS*, 373, L36
- van der Wel, A., Bell, E. F., van den Bosch, F. C., Gallazzi, A., & Rix, H. 2009, *ApJ*, 698, 1232
- van Dokkum, P. G., Franx, M., Kriek, M., Holden, B., Illingworth, G. D., Magee, D., Bouwens, R., Marchesini, D., et al. 2008, *ApJ*, 677, L5
- van Dokkum, P. G., Whitaker, K. E., Brammer, G., Franx, M., Kriek, M., Labbé, I., Marchesini, D., Quadri, R., et al. 2010, *ApJ*, 709, 1018
- Wuyts, S., Labbé, I., Schreiber, N. M. F., Franx, M., Rudnick, G., Brammer, G. B., & van Dokkum, P. G. 2008, *ApJ*, 682, 985